AIP | Journal of Applied Physics

Photoluminescence and resonant Raman scattering from ZnO-opal structures

V. V. Ursaki, I. M. Tiginyanu, V. V. Zalamai, V. M. Masalov, E. N. Samarov et al.

Citation: J. Appl. Phys. 96, 1001 (2004); doi: 10.1063/1.1762997
View online: http://dx.doi.org/10.1063/1.1762997
View Table of Contents: http://jap.aip.org/resource/1/JAPIAU/v96/i2
Published by the American Institute of Physics.

Related Articles

Optical analysis of doped ZnO thin films using nonparabolic conduction-band parameters
J. Appl. Phys. 111, 123507 (2012)

Structural transition in II-VI nanofilms: Effect of molar ratio on structural, morphological, and optical properties
J. Appl. Phys. 111, 113510 (2012)

Emission from a dipole-forbidden energy state in a ZnO quantum dot induced by a near-field interaction with a fiber probe
Appl. Phys. Lett. 100, 223110 (2012)

Effect of Lorentz local field for optical second order nonlinear susceptibility in ZnO nanorod
J. Appl. Phys. 111, 103112 (2012)

A comparative study of ultraviolet photoconductivity relaxation in zinc oxide (ZnO) thin films deposited by different techniques
J. Appl. Phys. 111, 102809 (2012)

Additional information on J. Appl. Phys.

Journal Homepage: http://jap.aip.org/
Journal Information: http://jap.aip.org/about/about_the_journal
Top downloads: http://jap.aip.org/features/most_downloaded
Information for Authors: http://jap.aip.org/authors

ADVERTISEMENT

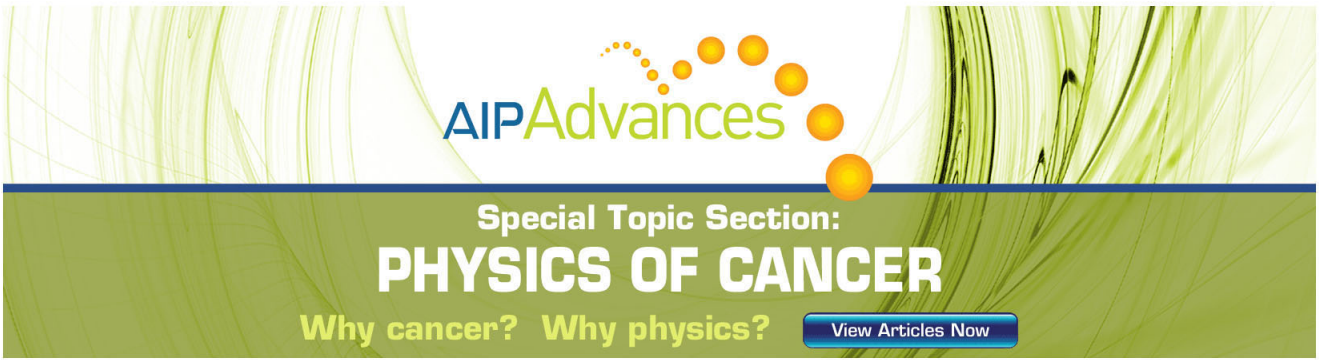

Downloaded 27 Jun 2012 to 161.111.180.103. Redistribution subject to AIP license or copyright; see http://jap.aip.org/about/rights_and_permissions

HTML ABSTRACT + LINKS

Photoluminescence and resonant Raman scattering from ZnO-opal structures

V. V. Ursaki, I. M. Tiginyanu,[a] and V. V. Zalamai
Laboratory of Low-Dimensional Semiconductor Structures, Institute of Applied Physics of the Academy of Sciences of Moldova, Technical University of Moldova, 2004 Chisinau, Moldova

V. M. Masalov, E. N. Samarov, and G. A. Emelchenko
Laboratory of Crystallization from High-Temperature Solutions, Institute of Solid State Physics, 142432 Chernogolovka, Moscow district, Russia

F. Briones
Centro Nacional de Microelectronica, Instituto de Microelectronica de Madrid, 28760 Madrid, Spain

(Received 5 January 2004; accepted 26 April 2004)

We study photoluminescence (PL) of ZnO-opal structures excited by a 351.1 nm laser line. The structures were fabricated by infiltration of ZnO from an aqueous solution of zinc nitrate into opal matrices. The emission spectrum of thick ZnO layers grown on the surface of bulk opals exhibits narrow PL bands associated with the recombination of bound and free-excitons. The free-exciton lines are discussed taking into account the polariton phenomena. The width of the excitonic lines (2–3 meV) along with their energy position is indicative of high quality and strain-free state of the layer. The emission from ZnO crystallites embedded into bulk opal is dominated by near band gap luminescence, a weak quantum confinement effect being observed for crystallites with sizes around 50 nm. Thin ZnO films grown on single-layer opals exhibit enhanced resonant Raman scattering, phonon confinement effects, and surface-related modes. Strong exciton-LO phonon and exciton-Fröhlich mode coupling in ZnO nanostructures is deduced from the analysis of multiphonon excitonic resonant Raman scattering. © *2004 American Institute of Physics.*
[DOI: 10.1063/1.1762997]

1. INTRODUCTION

The increasing interest in low-dimensional quantum systems such as arrays of quantum dots and wires realized in one-, two-, and three-dimensional (1D, 2D, and 3D) periodic structures is stimulated by their growing applications in nanoelectronics, optoelectronics, and photonics. Crystalline arrays of colloidal spheres represent one of the most promising templates for nanofabrication. 3D opal structures are ideal matrices for the purpose of filling with semiconductors, metals, magnetic materials, etc., in order to fabricate photonic crystals, arrays of quantum dots and other low-dimensional systems. The possibility to fabricate multilayer and single-layer ordered SiO_2 spheres on glass substrates has been recently demonstrated.[1,2] Growth of ordered metal and semiconductor structures inside the opal voids was reported[3–5] Note that single-layer opal structures can be used as nanomasks for the purpose of depositing different materials on substrates. This approach referred as ''nanosphere lithography'' enabled one recently to fabricate metal and semiconductor 2D arrays using polystyrene beads and molecular materials as nanomasks.[6] In many cases, the nanomasks must be resistant to thermal treatment, plasma etching, etc. Taking this into account, inorganic nanomasks and especially opal spheres are the most promising materials for nanolithography. The occurrence of physical properties in low-dimensional semiconductor materials-opal structures with potential exploitation in microelectronic and optoelectronic devices constitutes the motivation of the growing interest in these systems. For specific applications, the semiconductor component of these structures should also be resistant to hard environmental conditions. Zinc oxide (ZnO), a direct wide band gap (3.37 eV at 300 K) semiconductor with large exciton binding energy ($\sim$60 meV), is a promising material in this regard. The goal of this work was to fabricate different ZnO-opal structures and to study their radiative properties.

2. EXPERIMENTAL DETAILS

Silica opal spheres were synthesized through the hydrolysis of tetraethyl orthosilicate in water-ethanol solution in the presence of ammonium hydroxide following Stöber's method[7] with some modification of the component ratio.[2] 2D opal structures were prepared using the procedure of natural sedimentation combined with capillary contraction.[2] Multilayer and single-layer opal structures were fabricated by deposition on nearly vertical substrates during evaporation of the solvent. 3D opal matrices (bulk opals) were manufactured by natural sedimentation of the silica particles in a water suspension. After drying procedure at 150 °C, the samples were annealed at 1020 °C for 5 h. These technological steps resulted in opal structures exhibiting face-centered cubic lattice with the diameter of silica spheres $D_{SiO_2} \approx 220$ nm. This lattice possesses octahedral and tetrahedral voids with dimensions of $0.41 \times D_{SiO_2}$ and $0.22 \times D_{SiO_2}$, respectively. ZnO layers with the thickness ranging from 100

[a]Electronic mail: tiginyanu@mail.md

 © 2004 American Institute of Physics

Downloaded 27 Jun 2012 to 161.111.180.103. Redistribution subject to AIP license or copyright; see http://jap.aip.org/about/rights_and_permissions

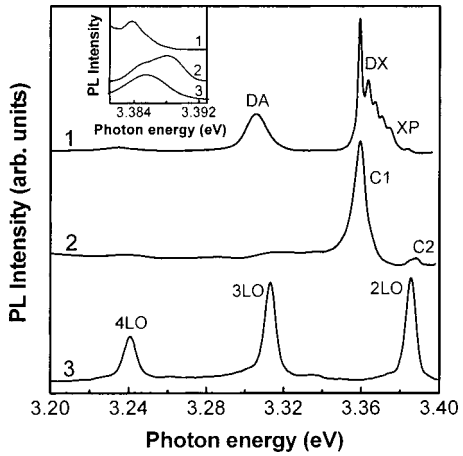

FIG. 1. Emission spectra of thick (500 nm) ZnO layer grown on bulk opal (curve 1), of ZnO nanocrystals embedded into bulk opal (curve 2), and of thin (100 nm) ZnO film deposited on single-layer opal (curve 3) measured at 10 K. Inserted are the normalized spectra in the high energy spectral region.

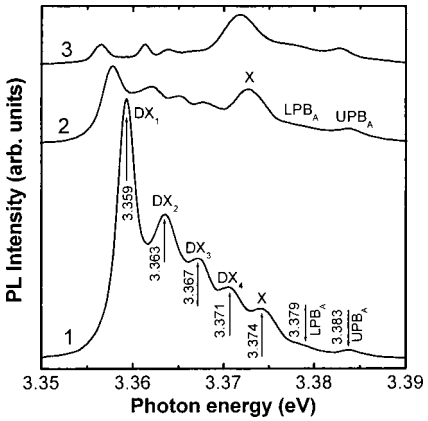

FIG. 2. PL spectra of thick ZnO layer grown on bulk opal measured at $T=20$ K (curve 1), at $T=50$ K (curve 2), and at $T=50$ K with additional excitation at power density of 5 W/cm^2 provided by the 514.5 nm line of a second Ar^+ laser (curve 3).

to 500 nm were grown on multilayer and single-layer opal structures using "wet" chemical deposition from a solution of $Zn(NO_3)_2 \cdot nH_2O$ followed by thermal decomposition of the zinc nitrate into zinc oxide. According to the solubility diagram of zinc nitrate in water, it exists only in the form of $Zn(NO_3)_2 \cdot nH_2O$ crystal hydrate, where the amount of water molecules varies from 9 to 1 in the temperature interval from $-32\,^\circ$C to $+70\,^\circ$C. The deposition was performed in the temperature interval from 55 to 70 °C, therefore zinc nitrate contains one-two water molecules. The same technology was used for the purpose of filling in voids in bulk opal with ZnO. The filling procedure consists of many cycles with the duration from 1.5 h for the first cycle to 20 h for the following cycles. After each cycle the surface of the opal was cleaned, dried, and the sample was thermally treated at definite temperatures from 450 to 600 °C to enable the decomposition of the nitrate into oxide. The filling of the opal voids with ZnO nanocrystals was monitored through the increase of the mass.

Photoluminescence (PL) was excited by the 351.1 nm line of an Ar^+ SpectraPhysics laser and analyzed in a quasi-backscattering geometry through a double spectrometer with 1200 grooves/mm gratings assuring a linear dispersion of 0.8 nm/mm. The signal from a FEU-106 photomultiplier with SbKNaCs photocathode working in a photon counting mode was introduced in an IBM computer via the IEEE-488 interface. The spectral resolution was better than 0.5 meV. The samples were mounted on the cold station of a LTS-22-C-330 workhorse-type optical cryogenic system. The excitation laser beam at 30-mW power was focused to a spot of about 2 mm in diameter resulting in the excitation power density of 1 W/cm^2. The beam power was increased gradually up to 100 mW and the beam diameter was reduced to 200 μm when studying the dependence of luminescence upon excitation power density.

3. RESULTS AND DISCUSSION

Figure 1 compares the unpolarized PL spectra at 10 K for 500-nm thick ZnO layer grown on bulk opal (curve 1), ZnO crystallites embedded in bulk opal (curve 2), and thin ($\sim$100-nm thick) ZnO film deposited on single-layer opal (curve 3). The PL spectrum of thick ZnO layers grown on bulk opals is dominated by the emission lines related to donor bound excitons (DX) and exciton polaritons (XP). A weaker PL band centered at 3.31 eV accompanied by its LO phonon replica at 3.24 eV is also observed in the spectrum.

Further we will consider the features of the exciton luminescence. Four PL bands related to donor bound excitons are located at 3.360, 3.364, 3.367, and 3.371 eV ($T=10$ K). The position of these lines corresponds to the emission related to donor-bound excitons usually observed in ZnO single crystals[8] and epitaxial layers.[9] With increasing temperature the luminescence related to donor-bound excitons decreases in intensity and, as a consequence of this, the exciton polariton luminescence becomes well resolved (see Fig. 2). Note that there is no consensus in the literature concerning the emission of *A* and *B* exciton polaritons. Obviously, to explain the free-exciton luminescence it is necessary to invoke the polariton picture. It is known that in strongly polar materials like ZnO transverse excitons couple with photons to form polaritons.[10,11] In such a case, the transverse-exciton dispersion mixes with the dispersion of photons to produce two new dispersion curves, known as upper polariton branch (UPB) and lower polariton branch (LPB). LPBs and UPBs can occur for excitons corresponding to three valence bands, namely *A*, *B*, and *C* ones. Some authors[8,9] consider that the PL bands at 3.376–3.378 eV are related to the *A* exciton polariton branches, while the band at 3.382–3.383 eV may be attributed to the *B* exciton polariton branches. We assume that the polariton emission in our ZnO layers can be interpreted on the basis of lower LPB_A and upper UPB_A polariton branches, as believed by Reynolds *et al.*[12] The 3.383 eV band can be assigned to the emission related to the UPB_A, while the PL band at 3.379 eV results from LPB_A. Apart from that, our layers exhibit a strong PL band at 3.374 eV. A similar band was observed by Reynolds *et al.*[12] in ZnO single crystals. Taking into account the energy position, the band involved may be attributed to donor-bound excitons. However, its properties are very similar to

Downloaded 27 Jun 2012 to 161.111.180.103. Redistribution subject to AIP license or copyright; see http://jap.aip.org/about/rights_and_permissions

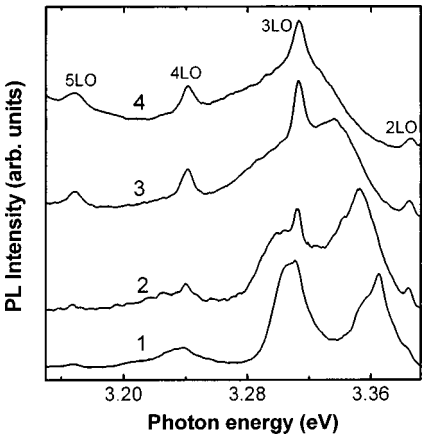

FIG. 3. Emission spectra of thick ZnO layer grown on bulk opal measured at temperatures 100 K (curve 1), 150 K (curve 2), 200 K (curve 3), and 250 K (curve 4).

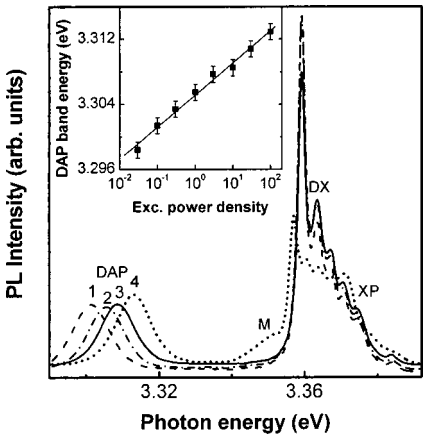

FIG. 4. The PL spectra of thick ZnO layer measured at $T=10$ K with different excitation power densities: 1–0.1 W/cm^2; 2–1 W/cm^2; 3–10 W/cm^2; 3–100 W/cm^2. The spectra are normalized to the intensity of DAP band. The insert shows the spectral peak position of the DAP emission as a function of the excitation power density. The solid line in the insert represents the linear least square fit of the experimental data.

the emission related to the LPB_A. With increasing temperature up to 70 K, the intensity of this band is constant, while the intensity of the bands related to donor-bound excitons sharply decreases (see Fig. 2). Apart from that, additional excitation of samples by 514.5 nm line of a second Ar^+ laser leads to the increase of the intensity of 3.374 eV band, while the bands related to donor-bound excitons decrease in intensity (see curve 3 in Fig. 2). The purpose of the second laser line is to excite additional free carriers in a two-step process, and thus partially screen the bound excitons. Additional excitation obviously stimulates the formation of exciton polaritons. The downward energy shift of both exciton polariton and bound exciton lines under dual excitation conditions is due to the free-carrier screening and band gap renormalization, as discussed elsewhere.[13] Therefore, the PL band at 3.374 eV labeled as X band[12] may be associated with the LPB_A, except that it must occur at lower **k** value, since it has a lower energy. More details concerning this band and its comparison with the X band observed in wurtzite GaN (Ref. 14) are presented by Reynolds *et al.*[12] The correspondence of bound exciton and exciton polariton lines in our layers with those inherent to single crystals indicates that the layers are free of strain. Note that this statement is supported by the position of very sensitive to strain E_2^{high} mode at 438 cm^{-1} in Raman scattering (RS) spectra, it coinciding with the position of respective mode in nonstressed ZnO single crystals.[15–17] Besides, the width of bound exciton lines in PL spectrum (2–3 meV), along with narrow lines observed in RS spectra (e.g., the width of the E_2^{low} mode is less than 1 cm^{-1}) are indicative of high crystalline quality of ZnO layers grown on opals.

With increasing temperature above 100 K the luminescence of ZnO layers grown on bulk opals decreases in intensity and remains free excitonic. Simultaneously with the decrease of luminescence intensity the emission related to the resonant Raman scattering reveals itself in the emission spectrum (see Fig. 3). The features of the resonant Raman scattering will be discussed below in connection with the emission from thin ZnO layers grown on single-layer opals.

As concerns the PL band at 3.31 eV, it is one of commonly occurring bands in high quality ZnO epitaxial films,[18–23], nanocrystalline thin films,[24] and ZnO rods.[25] Different recombination channels have been considered as the origin of this band. Primarily it was associated with the LO phonon replica of the free-exciton luminescence.[18–21,24] Some neutral acceptor-bound exciton emissions may also occur in this spectral range.[22,23] It is possible that the origin of this band depends upon the technological conditions of sample fabrication. The dependence of this band upon temperature and excitation power density in our layers is indicative of its connection with radiative recombination of free carriers via donor-acceptor pairs (DAP), in accordance with previous assumption.[25] The energy position of the band involved shifts to higher energies with increasing excitation power density (see Fig. 4), which is consistent with the saturation of distant pairs under increasing excitation, as expected for DAP recombination. An upward energy shift of 4 meV per one order of magnitude excitation power variation is deduced from the insert in Fig. 4. For completeness, one should note also the possibility for free-to-bound transitions shifting upwards with increasing excitation power density, as a result of band filling. However, the high shift gradient observed in our experiments seems to be unlikely for the free-to-bound case. Note that the DAP origin of the 3.31 eV band is confirmed by its temperature dependence. Within the explored temperature range, the 3.31 eV band moves towards the band gap, the rate of approach being close to $2kT$ (see Fig. 5). Free-to-bound transitions also move closer to the band edge with increasing temperature (due to the increase of the kinetic energy of free particles) but at much slower rate, given by $kT/2$.[26] The intensity of the band associated with DAP decreases considerably at temperatures higher than 180 K since the impurity with smaller binding energy involved in DAP transitions (more probable the donor impurity) becomes ionized with increasing temperature. Consequently, the rate of approach to the band edge deviates from $2kT$, possibly due to the predominance of free-to-bound

Downloaded 27 Jun 2012 to 161.111.180.103. Redistribution subject to AIP license or copyright; see http://jap.aip.org/about/rights_and_permissions

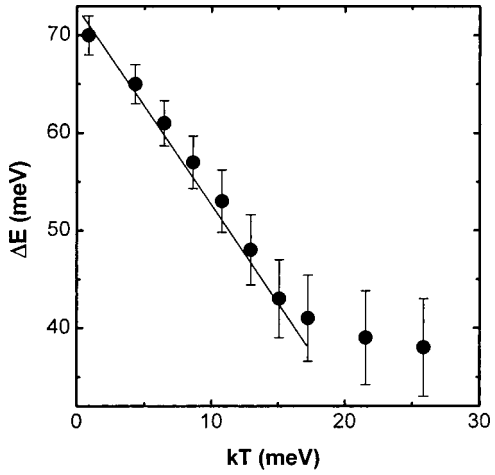

FIG. 5. The temperature dependence of the energy separation between the XP and DAP emission peaks, ΔE, in a ZnO layer. The solid line corresponds to the rate of approach of the DAP band to the band gap $d(\Delta E)/dT=2k$.

transitions at these temperatures. However, it is difficult to perform a reliable analysis at high temperatures due to strong overlapping of the bands and occurrence of 3LO resonant Raman scattering peak in the respective spectral range.

As one can see from Fig. 4, a new PL band at 3.35 eV labeled as M band emerges at excitation power densities higher than 100 W/cm^2. Similar band associated with a biexciton state was observed previously by Ko *et al.*[20] in high quality epitaxial ZnO films and studied in more detail by Yamamoto *et al.*[21] The M-band exhibits a superlinear dependence as a function of the excitation power density. The observation of biexciton emission at excitation intensity as low as 100 W/cm^2 was previously ascribed to the high quality of the material.[20] Unfortunately, the study of biexciton related emission with a cw excitation is difficult due to local heating of the sample at elevated excitation power densities indicated by the downward energy shift of the excitonic lines and by the sharp decrease in intensity of the bound exciton lines (curve 4 in Fig. 4). For this purpose it is necessary to use pulsed excitation[20,21] or other techniques such as two-photon reabsorption or two-photon Raman scattering.[27] Recently, biexcitonic states in ZnO crystals have been studied by means of four-wave mixing.[28]

The luminescence spectrum of ZnO nanocrystals embedded in bulk opals is dominated by two bands located at 3.360 and 3.388 eV (see curve 2 in Fig. 1). These two bands labeled as $C1$ and $C2$ are assumed to come from ZnO crystallites with different sizes. As discussed above, the opal lattice forms octahedral and tetrahedral voids inside with dimensions equaling 100 nm and 50 nm, respectively. The infiltration of ZnO into opal matrix leads to the formation of crystallites with respective sizes. Therefore, the PL band at 3.360 eV is attributed to crystallites with dimensions of 100 nm, while the band at 3.388 eV is assumed to come from ZnO crystallites with 50 nm dimensions. The upward frequency shift of the PL line in small crystallites is tentatively attributed to the quantum confinement effect. However, the crystallites with the size of 50 nm are rather big, and the fabrication of opals with the silica spheres smaller than 200 nm is required to reach conditions for pronounced quantum confinement phenomena. The PL band at 3.388 eV is superimposed onto the 2LO resonant Raman peak, as illustrated in the insert of Fig. 1. With increasing temperature above 100 K the luminescence of ZnO nanocrystals inside the opal decreases in intensity and the emission related to the resonant Raman scattering is observed like in ZnO layers grown on opals.

The emission spectrum of thin ZnO films deposited on single-layer opals is absolutely dominated by resonant Raman scattering (see curve 3 in Fig. 1). To explain the difference between the emission spectra of thick and thin ZnO layers the following two reasons can be considered: (i) the nanostructure enhanced resonant Raman scattering in thin layers, and (ii) the decrease of the luminescence efficiency due to the surface recombination. As shown recently,[29] ZnO layers with the thickness less than 100 nm deposited onto single-layer opals represent actually nanostructures consisting of crystallites with the sizes less than 50 nm deposited through the openings between the silica spheres, and crystallites with bigger sizes grown onto the upper surface of the opal spheres, i.e., the single-layer opal works as a nanomask in this case. On the other hand, the two types of crystallites that constitute the thin ZnO layers deposited on opals are practically identical to the types of crystallites embedded into bulk opals. The different emission properties of ZnO nanostructures involved imply different roles played by the crystallite surfaces. It is possible that the surface of the crystallites inside the bulk opal does not affect so strongly the luminescence as the surface of the crystallites grown on open single-layer opal does.

Resonance effects in light scattering from solids occur in the frequency regions of the electronic absorption bands. Resonant Raman scattering can be observed if the energy of the incoming or scattered photons matches real electronic states in the material. This results from the denominator in the Raman scattering cross section tending to zero. One refers to incoming and outgoing resonance, respectively (see, e.g., Ref. 30). Multiphonon scattering processes have been previously reported for single crystalline bulk ZnO,[31] and recently for ZnO films[24] and ZnO nanowires.[32] In all these cases the samples were excited by the 325 nm line of a He-Cd laser. The energy of this line is about 440 meV higher than the band gap of ZnO. It means that this is the case of incoming resonance, where the laser line is in resonance with an interband electronic transition, most probably between the $A_{5,6}$ valence band and Γ_1 conductance band as calculated theoretically[33,34] and measured experimentally[35] in wurtzite-type ZnO. In our case, the energy of the 351.1 nm Ar^+ laser line is about 90 meV higher than the ZnO band gap at 10 K, and the energy of the scattered photons matches the exciton energies. At 10 K the photon scattered by 2LO phonons matches the exciton energy and the 2LO peak proves to be stronger. With increasing temperature the exciton energy is redshifted and the photon scattered by 3LO phonons becomes in resonance with the excitons, as illustrated by curve 4 in Fig. 3. This is an first observation of multiphonon outgoing excitonic resonant Raman scattering in ZnO.

Downloaded 27 Jun 2012 to 161.111.180.103. Redistribution subject to AIP license or copyright; see http://jap.aip.org/about/rights_and_permissions

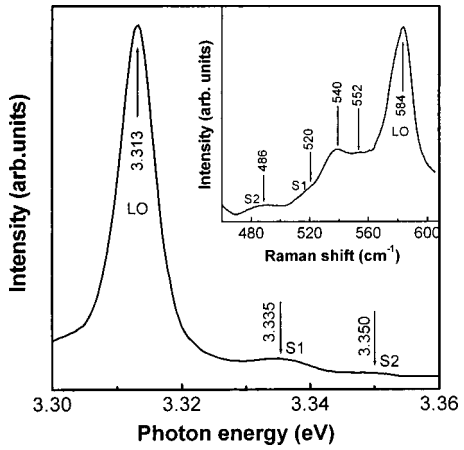

FIG. 6. The three-phonon resonant Raman scattering spectrum from a thin ZnO film deposited on single-layer opal. Inserted is a segment of the first-order Raman scattering spectrum in the vicinity of the LO phonons.

The strong Rayleigh scattering wing of the 351.1 nm laser line makes impossible the observation of one-phonon resonant Raman scattering. The analysis of the two-phonon scattering is also difficult due to the incidence of the 363.8 nm Ar^+ laser line on high energy wing of the 2LO peak. Therefore, we will focus our analysis at the three-phonon resonant Raman scattering illustrated in Fig. 6. For the purpose of comparison, the insert shows a segment of the first-order Raman scattering spectrum in the vicinity of the LO phonons. This spectrum was measured in backscattering geometry at room temperature under the excitation by 514.5 nm Ar^+ laser line using a Raman microscope.

Since the wurtzite structure of ZnO belongs to the C_{6v} space group, the zone center optical phonons are $A_1+E_1+2E_2$, and the polar symmetry A_1 and E_1 modes are the dominant ones in resonant Raman scattering. The peak in the resonant Raman spectrum is centered at 3.313 eV which implies that the phonon energy equals 72.5 meV. According to the first-order Raman scattering measurements,[15–17] this value is closer to the E_1(LO) phonon energy. The peak at 584 cm^{-1} in the insert also corresponds to the E_1(LO) phonon, although the asymmetrical low energy wing indicates to the contribution from the A_1(LO) phonon. Note that the E_1(LO) mode is forbidden in the backscattering geometry. The occurrence of this mode is likely due to the breakdown of the polarization selection rules caused by the use of the Raman microscope. The small scattering cross section for the A_1(LO) mode was previously explained taking into account the destructive interference between the Fröhlich interaction and the deformation potential contribution to the LO scattering in ZnO.[36]

The width of the 3LO line in the resonant Raman scattering spectrum (6.6 meV=53 cm^{-1}) is by a factor of 2 higher than the value obtained from the equation $\lambda(n\text{LO})=9n$ (cm^{-1}) for the phonon scattering linewidths[31] deduced from the contribution of mixed quasi-LO modes due to the anisotropic short-range forces in the uniaxial ZnO lattice.[37] The phonon line broadening, along with the contribution from A_1(LO) mode in ZnO nanowires[32] and nanoparticles,[38] were attributed to the phonon quantum confinement in ZnO nanostructures. Another characteristic feature of resonant Raman scattering spectra measured from ZnO-opal nanostructures is the presence of two weaker bands at 3.335 and 3.350 eV on the right-hand side of the 3LO peak. The deduced energies of the phonons participating in three-phonon processes (65.3 and 60.3 meV) strikingly correspond to the features at 520 and 486 cm^{-1}, marked as $S1$ and $S2$, respectively, in the nonresonant one-phonon spectrum. The other two bands at 540 and 552 cm^{-1} observed previously in bulk material and epilayers were assigned to the second-order Raman scattering.[15–17]

Finally, let us discuss the possible nature of the $S1$ and $S2$ bands. When the electromagnetic radiation propagates through nanostructures of polar materials, the polarization of the nanostructure entities in the electric field of the radiation results in the excitation of electrical dipoles vibrating at specific frequencies. These vibrations, not present in bulk material, give rise to new optical phonon modes located in the frequency gap between the bulk TO and LO optical phonons in binary compounds. The new optical modes, predicted by Fröhlich,[39] have been calculated for small ionic crystals of different morphologies by Fuchs and Kliewer[40,41] and have been observed in the infrared absorption and reflectivity spectra of powders by many authors. Fröhlich-type vibrational modes were extensively investigated in nanostructured III–V compounds with zincblende structure,[42] and recently were observed in wurtzite-type GaN columnar nanostructures.[43] According to calculations performed by Ruppin for small spherical crystals,[44] the efficiency of Raman scattering caused by Fröhlich modes is comparable with that caused by bulk LO and TO phonons only for crystallites with sizes smaller than 100 nm. We assume that the occurrence of $S1$ and $S2$ bands in both resonant and nonresonant Raman scattering is related to Fröhlich modes associated with ZnO crystallites with sizes of 50 nm and 100 nm. Since the crystallites are not spherical, the calculation of the position of surface modes in the Raman spectrum is a difficult task. On the other hand it is known that the smaller the size of the crystallites, the larger the separation between the LO and Fröhlich modes. In our opinion, the participation of Fröhlich modes in the excitonic multiphonon resonant Raman scattering is indicative of strong exciton-Fröhlich phonon coupling in wurtzite-type ZnO nanocrystals. Note that the interaction between surface-related phonons and confined electron-hole pairs was previously evidenced in resonance Raman scattering of GaP nanocrystals embedded into a glassy matrix.[45]

4. CONCLUSIONS

The results of this study demonstrate the possibility for growing high quality strain-free ZnO layers on opals from aqueous solutions of zinc nitrate. The same technology proves to be efficient for the purpose of filling in voids in bulk opals with ZnO nanocrystallites. The crystallites embedded into opal exhibit quantum confinement effects providing that the size of the silica spheres constituting the opal is less than 200 nm. The single-layer opals work as nanomask for the fabrication of ZnO nanostructures exhibiting

Downloaded 27 Jun 2012 to 161.111.180.103. Redistribution subject to AIP license or copyright; see http://jap.aip.org/about/rights_and_permissions

enhanced resonant Raman scattering, phonon confinement effects, and Fröhlich vibrational modes. Strong exciton-LO phonon and exciton-Fröhlich mode coupling in ZnO nanostructures is deduced from the analysis of multiphonon excitonic resonant Raman scattering.

ACKNOWLEDGMENTS

This work was supported by INTAS under Grant No. 01-0796. ISSP authors are grateful for the financial support received from the Russian Foundation for Basic Research (Project No. 01-02-97024) and from the Russian Federation Government under Contract No. 40.012.1.1.11.54.

[1] P. Jiang, J. F. Bertone, K. S. Hwang, and V. L. Colvin, Chem. Mater. **11**, 2132 (1999).
[2] V. M. Masalov, K. A. Aldushin, P. V. Dolganov, and G. A. Emel'chenko, Phys. Low-Dimens. Semicond. Struct. **5–6**, 45 (2001).
[3] V. N. Bogomolov, N. A. Feoktistov, V. G. Golubev, J. J. Hutchison, and I. M. Sorokin, J. Non-Cryst. Solids **266–269**, 1021 (2000).
[4] C. Diaz-Cuerra, J. Piqueras, V. G. Golubev, D. A. Curdyukiv, A. B. Pevtsov, and M. V. Zamoryanskaya, Appl. Phys. Lett. **77**, 3194 (2000).
[5] V. G. Golubev, D. A. Kurdyukov, A. V. Medvedev, A. B. Pevtsov, L. M. Sorokin, and J. J. Hutchison, Semiconductors **35**, 1320 (2001).
[6] Y. Xia, B. Gates, Y. Yin, and Y. Lu, Adv. Mater. (Weinheim, Ger.) **12**, 693 (2000).
[7] W. Stöber, A. Fink, and E. Bohn, J. Colloid Interface Sci. **26**, 62 (1968).
[8] S. F. Chichibu, T. Sota, G. Cantwell, D. B. Eason, and C. W. Litton, J. Appl. Phys. **93**, 756 (2003).
[9] S. W. Jung, W. I. Park, H. D. Cheong, G.-C. Yi, and H. M. Jang, Appl. Phys. Lett. **80**, 1924 (2002).
[10] S. I. Pekar, Zh. Eksp. Teor. Fiz. **33**, 1022 (1957) [Sov. Phys. JETP **6**, 785 (1958)].
[11] J. J. Hopfield and D. G. Thomas, Phys. Rev. **132**, 563 (1963).
[12] D. C. Reynolds, D. C. Look, B. Jogai, and T. C. Collins, Appl. Phys. Lett. **79**, 3794 (2001).
[13] D. C. Reynolds, D. C. Look, and B. Jogai, J. Appl. Phys. **88**, 5760 (2000).
[14] K. Torii, T. Deguchi, T. Sota, K. Sukuki, C. Chichibu, and S. Nakamura, Phys. Rev. B **60**, 4723 (1999).
[15] J. M. Calleja and M. Cardona, Phys. Rev. B **16**, 3753 (1977).
[16] F. Decremps, J. Pellicer-Porre, A. Marco Saitta, J.-C. Chervin, and A. Polian, Phys. Rev. B **65**, 092101 (2002).
[17] N. Ashkenov *et al.*, J. Appl. Phys. **93**, 126 (2003).
[18] Y. Chen *et al.*, J. Cryst. Growth **181**, 165 (1997).
[19] D. M. Bagnall, Y. F. Chen, M. Y. Shen, Z. Zhu, T. Goto, and T. Yao, J. Cryst. Growth **184/185**, 605 (1998).
[20] H. J. Ko, Y. F. Chen, T. Yao, K. Miyajima, A. Yamamoto, and T. Goto, Appl. Phys. Lett. **77**, 537 (2000).
[21] A. Yamamoto, K. Miyajima, T. Goto, H. J. Ko, and T. Yao, J. Appl. Phys. **90**, 4973 (2001).
[22] D. C. Look, D. C. Reynolds, C. W. Litton, R. L. Jones, D. B. Eason, and G. Cantwell, Appl. Phys. Lett. **81**, 1830 (2002).
[23] J. Chen and T. Fujita, Jpn. J. Appl. Phys., Part 2 **41**, L203 (2002).
[24] X. T. Zhang *et al.*, J. Phys. D **34**, 3430 (2001).
[25] B. P. Zhang, N. T. Binh, Y. Segawa, K. Wakatsuki, and N. Usami, Appl. Phys. Lett. **83**, 1635 (2003).
[26] D. M. Eagles, J. Phys. Chem. Solids **16**, 76 (1960).
[27] J. H. Hvam, G. Blattner, M. Reuscher, and C. Clingshirn, Phys. Status Solidi B **118**, 179 (1983).
[28] K. Hazu *et al.*, Phys. Rev. B **68**, 033205 (2003).
[29] A. N. Gruzintsev, V. T. Volkov, G. A. Emelchenko, I. A. Karpov, V. M. Masalov, G. M. Mikhailov, and E. E. Yakimov, Semiconductors **37**, 314 (2003).
[30] P. Y. Yu and M. Cardona, *Fundamentals of Semiconductors* (Springer, Berlin, 1996).
[31] J. F. Scott, Phys. Rev. B **2**, 1209 (1970).
[32] H. T. Ng, B. Chen, J. Li, J. Han, M. Meyyappan, J. Wu, S. X. Li, and E. E. Haller, Appl. Phys. Lett. **82**, 2023 (2003).
[33] P. Schroer, P. Kruger, and J. Pollmann, Phys. Rev. B **47**, 6971 (1993).
[34] W. R. L. Lambrecht, S. Limpijumnong, and B. Segall, MRS Internet J. Nitride Semicond. Res. **4S1**, G6.8 (1999).
[35] R. T. Girard, O. Tjernberg, G. Chiaia, S. Soderholm, U. O. Karsson, C. Wigren, H. Nylen, and I. Lindau, Surf. Sci. **373**, 409 (1997).
[36] R. H. Callender, S. S. Sussman, M. Selders, and R. K. Chang, Phys. Rev. B **7**, 3788 (1973).
[37] C. A. Arguello, D. L. Rousseau, and S. P. S. Porto, Phys. Rev. **181**, 1351 (1969).
[38] M. Rajalakshmi, A. K. Aror, B. C. Bendre, and S. Mahamuni, J. Appl. Phys. **87**, 2445 (2000).
[39] H. Fröhlich, *Theory of Dielectrics* (Clarendon, Oxford, 1949).
[40] R. Fuchs and K. L. Kliewer, Phys. Rev. A **140**, 2076 (1965).
[41] R. Fuchs and K. L. Kliewer, J. Opt. Soc. Am. **58**, 319 (1967).
[42] See for instance I. M. Tiginyanu, G. Irmer, J. Monecke, and H. L. Hartnagel, Phys. Rev. B **55**, 6739 (1997); A. Sarua, G. Irmer, J. Monecke, I. M. Tiginyanu, C. Schwab, J.-J. Grob, and H. L. Hartnagel, J. Appl. Phys. **88**, 7006 (2000); V. V. Ursaki, I. M. Tiginyanu, P. C. Ricci, A. Anedda, E. V. Foca, and N. N. Syrbu, J. Phys.: Condens. Matter **13**, 4579 (2001).
[43] I. M. Tiginyanu, A. Sarua, G. Irmer, J. Monecke, S. M. Hubbard, D. Pavlidis, and V. Valiaev, Phys. Rev. B **64**, 233317 (2001).
[44] R. Ruppin, J. Phys. C **8**, 1969 (1975).
[45] Al. L. Efros, A. I. Ekimov, F. Kozlowski, V. Petrova-Koch, H. Schmidbaur, and S. Shumilov, Solid State Commun. **78**, 853 (1991).

Downloaded 27 Jun 2012 to 161.111.180.103. Redistribution subject to AIP license or copyright; see http://jap.aip.org/about/rights_and_permissions